JOC The Journal of Organic Chemistry

Note

pubs.acs.org/joc

Replacing Phenyl Ring with Thiophene: An Approach to Longer Wavelength Aza-dipyrromethene Boron Difluoride (Aza-BODIPY) Dyes

Xinfu Zhang, Haibo Yu, and Yi Xiao*

State Key Laboratory of Fine Chemicals, Dalian University of Technology, West Campus, 2 Linggong Road, Dalian 116012, China

Supporting Information

ABSTRACT: In the orignial 1,3,5,7-tetraphenyl aza-BODIPY, replacing the phenyl rings with thiophene achieved significant bathochromic shifts. One of the target molecules, **DPDTAB**, emitting strong NIR fluorescence with a quantum yield of 0.46 in acetonitrile, is a very competitive NIR fluorophore.

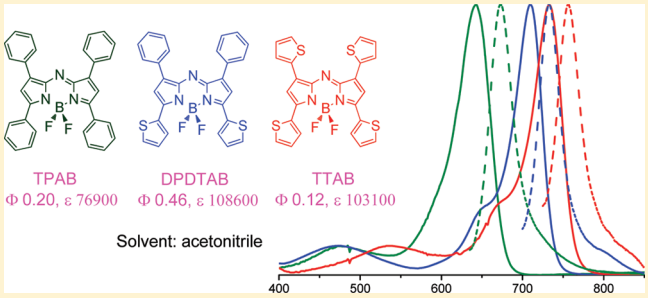

Bright prospects for near-infrared (NIR) fluorescent dyes in life sciences have been recognized.[1] These dyes will play more and more important roles in biological sensing and imaging, photodynamic therapy, etc. because NIR light can penetrate biological tissues more deeply and noninvasively than UV−vis light.[2] The application fields call for the exploration of a large number of NIR dyes with excitation/emission at various wavelengths in the NIR region. Aza-dipyrromethene boron difluoride (aza-Bodipy) dyes exhibiting favorable photochemical and photophysical properties attract considerable attention.[3−6] So far, most of these derivatives are actually tetraphenyl aza-BODIPYs, having four phenyl groups directly substituted on the 1, 3, 5, and 7 positions of the aza-BODIPY core (unknown structure, Figure 1). The absorption and emission maxima of the precursor tetraphenyl aza-BODIPY (**TPAB** shown in Figure 1) are below 700 nm. Generally, two approaches are adopted to move the spectra bands into the NIR region. One is to modify on the initial phenyl groups, such as introducing the electro-donating group, and extending conjugation length.[7,8] The other is to fuse the 3- and 5-phenyl groups to the aza-BODIPY core by the formation of six-membered rings,[9,10] which in essence, is to decrease the steric clash-generated torsion angles between the phenyl rings and the plane of the central chromophore. The additional NIR bathochromic shifts observed in these "constrained" molecules can be ascribed to the better electron delocalization due to the enhancement of coplanarity of the 3- and 5-phenyl groups with the aza-BODIPY core. Obviously, the existence of torsion angles is one of the important issues, and how to address it becomes crucial for developing longer wavelength aza-BODIPY. Herein, we propose replacing the common phenyl groups by smaller five-membered rings for the sake of releasing the steric clash (Figure 1). Thiophene is the first choice because many materials containing thiophene in the structures exhibit a wide range of interesting optical properties.[11,12] In addition, electron-rich thiophene may also play a similar role as the electron-donating phenyl substituent favoring bathochromic shift. In fact, thiophene has been introduced into BODIPY dyes, and they show clear red shift in both absorption and emission.[13] However, there has been no report that thiophenes are introduced into aza-BODIPY.

For this investigation, diphenyldithienyl aza-BODIPY (**DPDTAB**) and tetrathienyl aza-BODIPY (**TTAB**) were designed, and the tetraphenyl aza-BODIPY (**TPAB**) was used as the reference. Initially, DFT calculations were carried out for rationalizing structure−property relationships,[13,14] with part of the data listed in Table 1. In **DPDTAB** and **TTAB**, the torsion angles between the thienyl rings and the aza-Bodipy core are remarkably smaller than those counterparts between the phenyl rings and the aza-Bodipy core in **TPAB**. While all three compounds have almost the same LUMO energy, HOMO levels of **TTAB** and **DPDTAB** are 0.28 and 0.25 eV higher than that of **TPAB**, which means smaller energy transitions and bathochromic shifts for **DPDTAB** and **TTAB** compared with **TPAB**. Calculated absorption and emission shows general trend of red shift, and these values are close to the experimental result. Another purpose of the quantum calculation is to estimate the lowest lying singlet excited state, which is responsible for the emissive property of the fluorophore. According to the quantum mechanics selection rule, emissive properties (as well as the excitation) of a dye can be evaluated by the symmetry and the overlapping of the molecular orbitals (MOs), the change of the spin state, and the oscillator strength (f) of the electronic transitions, etc.[15−17] The DFT calculation demonstrates **DPDTAB** bearing higher $S_1 \leftarrow S_0$ transition

Received: July 10, 2011
Published: November 23, 2011

dx.doi.org/10.1021/jo201413b | J. Org. Chem. 2012, 77, 669−673

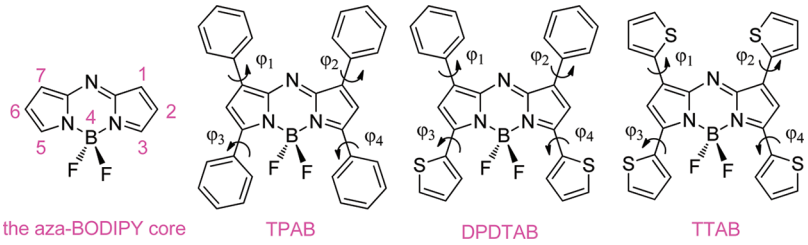

Figure 1. Structures of aza-BODIPY core, **TPAB**, **DPDTAB**, and **TTAB**. φ_1–φ_4 are torsion angles between the aromatic rings and the plane of the central chromophore.

Table 1. DFT Calculation Results[a]

	φ_1[b]	φ_2	φ_3	φ_4	λ_{abs}[c] (nm)	λ_{em}[c] (nm)	f[d]	HOMO/LUMO (eV)
TPAB	24.45	29.98	39.35	33.77	614	682	0.5082	−5.58/−3.42
DPDTAB	24.62	40.91	6.25	24.05	646	696	0.6230	−5.34/−3.41
TTAB	2.98	22.44	17.65	26.59	710	770	0.4407	−5.30/−3.45

[a]Calculations were carried out using the Turbomole program suite, employing the B3LYP functional. [b]φ_1–φ_4 stand for torsion angles between the aromatic rings and the plane of the central chromophore. [c]Stands for calculated absorption and emission separately. [d]Oscillator strength of $S_1 \leftarrow S_0$ transition.

Scheme 1. Synthetic Procedures for DPDTAB and TTAB[a]

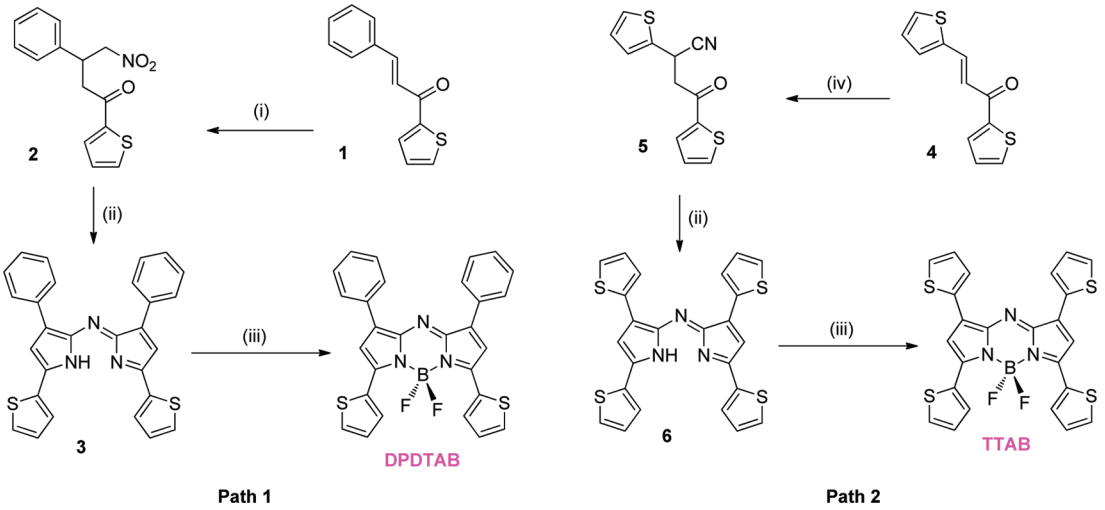

[a]Reagents and conditions: (i) CH_3NO_2, NEt_3, MeOH, reflux 10 h; (ii) NH_4OAc, BuOH, reflux, 24 h; (iii) $BF_3{\cdot}OEt_2$, $NiPr_2Et$, CH_2Cl_2, 25 °C, overnight; (iv) KCN, acetic acid, ethanol, 35 °C.

oscillator strength (f) of 0.6230 than that of **TPAB** (0.5082). This means the reverse transition, that is, the $S_1 \rightarrow S_0$ transition, is also fully allowed; thus, this dye is potentially fluorescent. As for TTAB, the lower f value (0.4407) may mean weaker fluorescence.

Encouraged by the positive results of the DFT calculations, we synthesized the two target compounds via different paths, as shown in Scheme 1. Path 1 was the most often adopted procedure to synthesize tetraphenyl aza-BODIPY derivatives, by which **DPDTAB** with two thienyl groups were obtained without problems. However, in the second step of this path, nitrous acid will be released as a byproduct, according to the suggested mechanism. To avoid the potential risk of oxidative damage to the electron-rich thienyl moieties, for the synthesis of **TTAB** with four thienyl groups, we decided to adopt an alternative route which did not use or generate oxidative agents; this route was not as commonly used as path 1 in the previous preparation of tetraphenyl aza-BODIPY derivatives, perhaps because of the use of toxic KCN. Through path 2, desirable **TTAB** were obtained, although the yield still needs to be improved.

Single-crystal X-ray structures of **DPDTAB** and **TTAB** are shown in Figure 2, and the data of the torsion angles were listed in Table 2. For comparison with torsion angles of dimethoxytetraphenyl aza-BODIPY, **DMTPAB**[18] was cited as a reference. The target molecules **DPDTAB** and **TTAB** bear much smaller torsion angles (Table 2) than **DMTPAB**, agreeing with the tendency predicted by DFT calculation. In **TTAB**, all the four torsion angles are smaller than 10°, indicating **TTAB**'s conjugation structure are totally planar. In **DPDTAB**, φ3 and φ4 are smaller than 1° which are almost negligible. Contrastingly, in **DMTPAB**, φ3 and φ4 between the phenyl groups and the central plane are as large as 39° and 34°, respectively. It is also found that in each of the three compounds, φ1 is quite different from φ4, and φ3 is quite different from φ4. For example, in **TTAB**, φ3 is around 9°, but φ4 is only 1°. This interesting phenomenon reveals that the "seemingly symmetric" structures of these aza-BODIPYs are

dx.doi.org/10.1021/jo201413b | J. Org. Chem. 2012, 77, 669–673

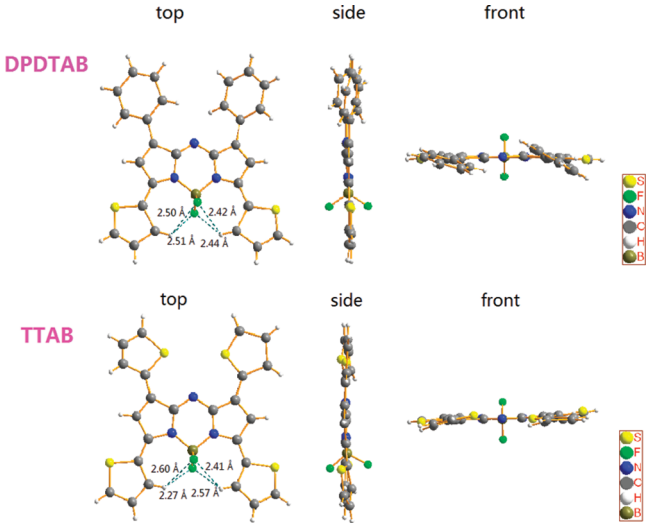

Figure 2. X-ray crystal structures of **DPDTAB** and **TTAB**.

Table 2. Torsion Angles in DPDTAB,[a] TTAB and Reference Compound DMTPAB[18] Obtained from Crystallography

	φ_1	φ_2	φ_3	φ_4
DPDTAB	18.552	25.723	0.058	0.589
TTAB	5.166	9.728	8.714	0.955
DMTPAB	14.426	7.291	38.758	33.857

[a]**DMTPAB** stands for dimethoxytetraphenyl aza-BODIPY cited from reference.[18].

actually nonsymmetric. As is reported in tertraphenyl aza-BODIPY, phenyls at the 3- and 5-positions were restricted from free rotation owing to the steric hindrance induced by the C−H...F interactions.[19] In our cases, the values of C−H···F distance for **DPDTAB** and **TTAB** were measured. The the average value for **DPDTAB** was measured as 2.47 Å, and for **TTAB**, it was 2.46 Å. These values are both less than the sum of the van der Waals radii for hydrogen and fluorine (2.62 Å), which implies that an interaction between these atoms is likely. The interaction will help to keep the whole molecule planar.

Subsequently, photophysical properties were measured in solvents with different polarity. The absorption and emission spectra in acetonitrile are recorded in Figure 3, and the data are

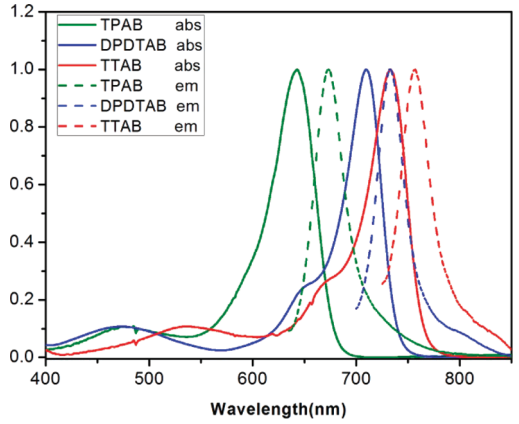

Figure 3. Normalized absorption (solid line) and emission (dashed line) for **TPAB** (green), **DPDTAB** (blue), and **TTAB** (red) in acetonitrile.

listed in Table 3. In general, thienyl-bearing **DPDTAB** and **TTAB** show siginificant bathochromic shifts of 60−90 nm in both the absorption and emission, compared with those of **TPAB**. When two phenyls group on the 3- and 5-positions of **TPAB** are replaced by thienyl groups to form **DPDTAB**, a 67 nm red shift in absorption and a 58 nm shift in emission are generated. However, further introducing two more thienyl groups on the 1- and 7-positions to get **TTAB** leads to only an extra 23 nm shift compared to **DPDTAB** for absorption and 24 nm for fluorescence. As a result, thiophene rings at the 3- and 5-positions contribute more pronouncedly to the bathochromic shifts than those on the 1- and 7-positions. A similar phenomenon happens to previous tetraphenyl aza-BODIPY too; that is, modifications on the 3- and 5-phenyl rings affect the optical properties more than on the 1- and 7-phenyl rings, which can be concluded as the *o*-pyrollic position inducing a better delocalization.[6] **DPDTAB** exhibits strong NIR emission with a quantum yield of 0.46, which is a rather high value for NIR dyes. It is counterintuitive that introducing a heavy atom (to some extent sulfur is heavy atom) could give rise to fluorescence quantum yield increment. However, it is not easy to rationalize the effect of the presence of thiophene groups in the photobehavior of fluorophores since all (radiative, reactive and nonradiative) relaxations processes can be perturbed by the heteroatom. It is actually competing between nonradiative deactivation processes and fluorescence emission.[21,22] For better understanding of this, fluorescence lifetimes of these three compounds were measured (Figure 4 and Table 3). Both **DPDTAB** and **TTAB** bear longer fluorescence lifetimes compared to **TPAB**, 3.56 ns for **DPDTAB** and 2.23 ns for **DTAB**. Further, both radiative (K_r) and nonradiative (K_{nr}) decay rates (in relation with Φ_f and τ) of **DPDTAB** are lower than that of **TPAB**, but the K_{nr} decreases more significantly. In other words, the weight of the radiative channel in the total decay of **DPDTAB** gets bigger. Therefore, the increase in quantum of **DPDTAB** is related mostly to the smaller nonradiative decay rate. However, the **TTAB**, with longest absorption/emission wavelength, shows much lower fluorescence quantum yield of 0.12. This is also a combined effect of K_r and K_{nr}. In this case, the K_r is much smaller, and the K_{nr} is much bigger than those of **TPAB**, respectively. Enhanced IC (internal conversion) by lower energy gap is one pathway for nonradiative transition.

In addition, the absorption spectra showed only a small sensitivity to solvent polarity. For example, the λ_{abs} and λ_{em} of **DPDTAB** in DMSO is only red-shifted by about 10 nm when compared to that in CH_2Cl_2 (Table 4). All of the other data hardly show any different ether. The same phenomenon happened to **TTAB**. This highly favorable emission wavelengths and insensitivity to solvent polarity are strongly indicative of future applications in biotechnology.

Cyclic voltammetry was used to probe the electronic effects of different aryl substituent on the aza-BODIPY chromophore, with data listed Table 4. All three aza-BODIPYs display one reversible oxidation wave and two reversible reduction waves (Supporting Information). HOMO and LUMO values have been evaluated and are listed in Table 5. These values share the same tendency with the computed ones. HOMO values increase from −6.04 eV to about −5.83 eV, and LUMO values keep constant at about −4.23 eV. Lower band gaps are obtained for **DPDTAB** and **TTAB** due to the introduction of electronic donating thiophene rings.

dx.doi.org/10.1021/jo201413b | *J. Org. Chem.* 2012, 77, 669−673

Table 3. Photophysical Properties of TPAB, DPDTAB and TTAB in acetonitrile

compd	λ_{abs} (nm)	$\lambda_{abs\text{-}cal}$ [a] (nm)	ε (M^{-1} cm^{-1})	λ_{em} (nm)	$\lambda_{em\text{-}cal}$ [a] (nm)	Φ_f [b]	τ [c] (ns)	K_r [d] (10^8 s^{-1})	K_{nr} [d] (10^8 s^{-1})
TPAB	643	614	76900	673	682	0.22	0.78	2.56	10.26
DPDTAB	710	646	108600	732	696	0.46	3.56	1.29	1.52
TTAB	733	710	103100	757	770	0.11	2.23	0.54	3.95

[a]Stands for calculated absorption and emission separately. [b]Reported 3,5-bis*p*-methoxyphenyl)-1,7-bis*p*-bromophenyl)za-BODIPY (Φ_f 0.42, in tolunene) was used as standard.[20] [c]Fluorescence lifetime was determined by using Edinburgh OB 920 Fluorescence/Phosphorescence lifetime spectrometer. [d]Radiative (K_r) and nonradiative (K_{nr}) decay rates.

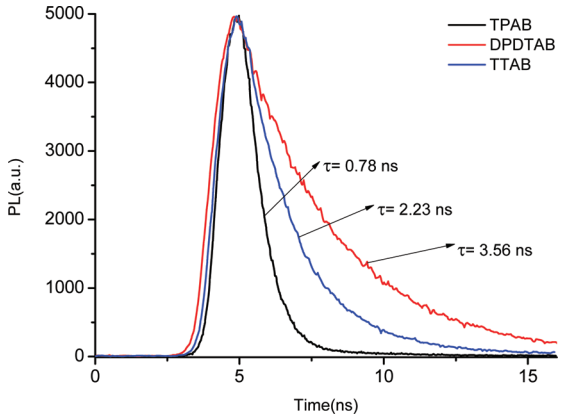

Figure 4. Fluorescence lifetime hyperbolic curves of **TPAB** (black line), **DPDTAB** (red line), and **TTAB** (blue line) in acetonitrile.

In conclusion, by replacing the phenyl rings with thiophene in the original 1,3,5,7-tetraphenyl aza-BODIPY, significant bathochromic shifts were achieved, suggesting a feasible strategy to develop NIR dyes. The data of X-ray crystalgraphy, DFT calculations, and electrochemical investigations ascribed the origin of bathochromic shift to the smaller torsion angles and higher electron donating capability of thienyl against phenyl units introduced to aza-BODIPY core. This work also provided a very competitive NIR fluorophore, **DPDTAB**, which emits strong NIR fluorescene with a quantum yield of 0.46 in acetonitrile. Our current work is focused on enhancing fluorescence quantum yield by restricting the rotation of thiophene rings and improving the water solubility for application in biotechnology.

EXPERIMENTAL SECTION

Reference compounds **TPAB**[7] and **DMTPAB**[20] and the starting materials thienyl-3-phenylprop-2-en-1-one (**1**) and thienyl-3-thienyl-prop-2-en-1-one (**4**)[23] were synthesized according to literature procedures.

Phenyl 4-Nitro-3-thienylbutan-1-one (2). A solution of thienyl-3-phenylprop-2-en-1-one(2b) (3.5 g, 16.4 mmol), triethyl-amine (7 mL, 48.4 mmol), and nitromethane (3.5 mL, 65.4 mmol) in methanol (20 mL) was heated under reflux for 8 h. The reaction was cooled to room temperature and acidified with HCl to pH 4. The methanol was removed, and the resulting oil was portioned between CH_2Cl_2 (50 mL) and water (50 mL). The aqueous layer was washed with CH_2Cl_2 (2 × 50 mL), and the combined organic fractions were dried over anhydrous magnesium sulfate. The solvent was removed, and the resulting yellow oil product was use in next without further purification (4.25 g, 95%): ^{1}H NMR (400 MHz, $CDCl_3$) δ 7.66 (d, J = 4.4 Hz, 1H), 7.61 (d, J = 5.2 Hz, 1H), 7.32−7.22 (m, 5H), 7.08 (t, J = 4.0, 4.0 Hz, 1H), 4.83−4.78 (m, 1H), 4.70−4.85 (m, 1H), 4.22−4.15 (m, 1H), 3.42−3.29 (m, 1H); ^{13}C NMR (100 MHz, $CDCl_3$) δ 189.8, 143.6, 138.9, 134.4, 132.4, 129.1, 128.9, 128.4, 127.9, 127.5, 42.2, 34.58; m/z (TOF-MS-EI) calcd $[M - NO_2]^+$ for $C_{14}H_{13}OS$ 229.0687, found 229.0692.

Table 5. Electrochemical Data of TDAB, DPDTAB, and TTAB in CH_2Cl_2 (Scan Rate 100 mV s^{-1})

	E_g [a] eV)	$E_{red,1/2}$ (V) vs ferrocene	HOMO[b]/LUMO[c](eV)
TDAB	1.81	−0.85	−6.04/-4.23
DPDTAB	1.68	−0.84	−5.92/-4.24
TTAB	1.61	−0.86	−5.83/-4.22

[a]Optical bandgap, $E_g = hc/\lambda_c$, h is Planck's constant, c is the speed of light, λ_c is edge absorption. [b]HOMO = $-(E_g - LUMO)$. [c]Based on the assumption that the energy of Fc/Fc^+ is 5.08 eV relative to vacuum.

Thienyl 4-Cyano-3-phenylbutan-1-one (5). A solution of **4** (6.6 g, 29.5 mmol) in ethanol was stirred at 35 °C. Acetic acid (1.8 mL) was added and the mixture stirred for 15 min. To the above solution was added KCN (3.7 g, 57 mmol) in water (10 mL). After all of the raw material was consumed, the reaction mixture was portioned between CH_2Cl_2 (100 mL) and water (100 mL). The aqueous layer was washed with CH_2Cl_2 (2 × 50 mL), and the combined organic fractions were dried over anhydrous magnesium sulfate. The solvent was removed, and the resulting yellow oil product was purified by column chromatography on silica gel eluting with CH_2Cl_2 and mineral ether (v/v = 1:1). White solid was collected (2.6 g, 36%): mp 86.3−88.0 °C; ^{1}H NMR (400 MHz, $CDCl_3$) δ 7.73 (d, J = 4.0 Hz, 1H), 7.70 (d, J = 4.8 Hz, 1H), 7.26 (d, J = 5.2 Hz, 1H), 7.15 (t, J = 4.0, 4.8 Hz, 1H), 6.97 (t, J = 5.2 Hz, 1H), 4.85 (t, J = 4.0 Hz, 1H), 3.70 (dd, J = 20, 8 Hz, 1H), 3.57 (dd, J = 20, 8 Hz, 1H); ^{13}C NMR (100 MHz, $CDCl_3$) δ 187.0, 142.6, 136.7, 134.9, 132.7, 128.4, 127.2, 126.8, 126.0, 119.5, 77.4, 77.1, 76.8, 44.8, 27.3; m/z (TOF-MS-ES) calcd M^+ for $C_{12}H_9NOS_2$ 247.0126, found 247.0133.

Azadipyrromethene (3). A solution of **2** (2 g, 7.33 mmol) and ammonium acetate (8.46 g, 109.89 mmol) in butanol was heated under reflux for 24 h. After the solution was cooled to room temperature, the solvent was concentrated to a quarter of its original volume and filtered, and the isolated solid was washed with ethanol to yield a dark blue-black solid. The crude product was used in the next step without any further purification (0.20 g, 12%): mp 281.1−284.5 °C; ^{1}H NMR (400 MHz, $CDCl_3$) δ 8.03 (d, J = 7.2 Hz, 4H), 7.60 (s,

Table 4. Effects of the Solvent Polarity on Photophysical Properties of DPDTAB

sovent	λ_{abs} (nm)	λ_{em} (nm)	ε (M^{-1} cm^{-1})	φ	τ (ns)	K_r (10^8 s^{-1})	K_{nr} (10^8 s^{-1})
CH_2Cl_2	717	739	114500	0.47	3.71	1.27	1.43
tluene	720	741	120700	0.44	3.70	1.19	1.51
THF	717	738	120500	0.46	3.22	1.43	1.68
aetonitrile	710	732	108600	0.46	3.56	1.29	1.52
DMSO	727	751	112900	0.42	3.36	1.25	1.73

dx.doi.org/10.1021/jo201413b | J. Org. Chem. 2012, 77, 669−673

2H), 7.50 (d, J = 4.0 Hz, 2H), 7.40 (d, J = 7.2, 4H), 7.35 (d, J = 6.8 Hz, 2H), 7.20 (s, 2H), 7.06 (s, 2H); ^{13}C NMR (100 MHz, $CDCl_3$) δ 149.8, 144.9, 137.1, 134.4, 133.99, 133.1, 133.0, 132.9, 131.5, 129.9, 129.7, 129.4, 128.1, 116.22; m/z (TOF-MS-ES) calcd $[M + H]^+$ for $C_{28}H_{19}N_3S_2$ 462.1099, found 462.1103.

Azadipyrromethene (6). A solution of **5** (2 g, 8.10 mmol) and ammonium acetate (8.28 g, 107.55 mmol) in butanol was heated under reflux for 24 h. After thesolution was cooled to room temperature, the solvent was concentrated to a quarter of its original volume and filtered, and the isolated solid was washed with ethanol to yield a dark blue-black solid. The crude product was used in the next step without any further purification (95.75 mg, 5%): mp >300 °C; m/z (TOF-MS-ES) calcd $[M + H]^+$ for $C_{24}H_{16}N_3S_4$ 474.0227, found 474.0229. ^{1}H NMR and ^{13}C NMR spectra were not available due to the extremely poor solubility of **6** in $CDCl_3$ and DMSO-d_6, etc.

DPDTAB. A dried flask was charged with **3** (200 mg,0.43 mmol) and flushed with nitrogen. Dry dichloromethane (200 mL) and dry diisopropylethylamine (0.77 mL, 4.3 mmol) were then added. The solution was stirred at 25 °C for 15 min, and then $BF_3{\cdot}OEt_2$ (0.83 mL, 6.5 mmol) was added. After being stirred at 25 °C for 24 h, the mixture was washed with water, and the organic layer was dried over magnesium sulfate and concentrated in vacuo to give the target compound. Purification by column chromatography on silica gel eluting with CH_2Cl_2 provided a dark brown solid (204.90 mg, 93%): mp >300 °C; ^{1}H NMR (400 MHz, $CDCl_3$) δ 8.38 (d, J = 3.6 Hz, 1H), 8.05 (d, J = 7.2 Hz, 2H), 7.64 (d, J = 4.8 Hz, 1H), 7.48−7.38 (m, 3H), 7.27 (d, J = 4.0 Hz, 1H), 7.18 (s, 1H); ^{13}C NMR (100 MHz, $CDCl_3$) δ 149.8, 145.6, 142.8, 134.1, 133.2, 133.1, 133.0, 132.1, 131.7, 129.8, 129.4, 129.2, 128.5, 118.6; m/z (TOF-LD) calcd M^+ for $C_{28}H_{18}N_3F_2S_2B$ 509.1003, found 509.1001.

TTAB. A dried flask was charged with **6** (50 mg, 0.11 mmol) and flushed with argon. Dry dichloromethane and dry diisopropylethylamine (0.19 mL, 1.1 mmol) were then added. The solution was stirred at 25 °C for 15 min, and then $BF_3{\cdot}OEt_2$ (0.83 mL, 15 equiv) was added. After being stirred at 25 °C for 24 h, the mixture was washed with water, and the organic layer was dried over magnesium sulfate and concentrated in vacuo to give the target compound. Purification by column chromatography on silica gel eluting with CH_2Cl_2 provided a dark brown solid (53.87 mg, 98%): mp >300 °C; ^{1}H NMR (400 MHz, $CDCl_3$) δ 8.34 (d, J = 3.6 Hz, 1H), 7.92 (d, J = 3.6 Hz, 1H), 7.62 (d, J = 4.8 Hz, 1H), 7.56 (d, J = 4.8 Hz, 1H), 7.20 (t, J = 4.0, 4.8 Hz, 1H), 7.07 (s, 1H); ^{13}C NMR (100 MHz, $CDCl_3$) δ 144.9, 134.4, 133.9, 133.0, 131.5, 129.9, 129.7, 129.4, 128.1, 116.2; m/z (TOF-MS-EI) calcd M^+ for $C_{24}H_{14}N_3F_2S_4B$ 521.0132, found 521.0134.

■ ASSOCIATED CONTENT

Ⓢ Supporting Information

Experimental procedures, characterization data, X-ray structures, crystal data, and computational details. This material is available free of charge via the Internet at http://pubs.acs.org.

■ AUTHOR INFORMATION

Corresponding Author

*E-mail: xiaoyi@dlut.edu.cn.

■ ACKNOWLEDGMENTS

We thank the NSF of China (Nos. 20876022) and the Fundamental Research Funds for the Central University (DUT10ZD114) for financial support.

■ REFERENCES

(1) Kiyose, K.; Kojima, H.; Nagano, T. *Chem. Asian J.* **2008**, *3*, 506−515.
(2) Frangioni, J. V. *Curr. Opin. Chem. Biol.* **2003**, *7*, 626−634.
(3) Allik, T. H.; Hermes, R. E.; Sathyamoorthi, G.; Boyer, J. H. *Proc. SPIE-Int. Soc. Opt. Eng.* **1994**, *2115*, 240−248.
(4) Murtagh, J.; Frimannsson, D. O.; O'Shea, D. F. *Org. Lett.* **2009**, *11*, 5386−5389.
(5) Palma, A.; Tasior, M.; Frimannsson, D. O.; Vu, T. T.; Méallet-Renault, R.; O'Shea, D. F. *Org. Lett.* **2009**, *11*, 3638−3641.
(6) Bouit, P.-A.; Kamada, K.; Feneyrou, P.; Berginc, G.; Toupet, L.; Maury, O.; Andraud, C. *Adv. Mater.* **2009**, *21*, 1151−1154.
(7) Gorman, A.; Killoran, J.; O'Shea, C.; Kenna, T.; Gallagher, W. M.; O'Shea, D. F. *J. Am. Chem. Soc.* **2004**, *126*, 10619−10631.
(8) Bellier, Q.; Pégaz, S.; Aronica, C.; Guennic, B. L.; Andraud, C.; Maury, O. *Org. Lett.* **2011**, *13*, 22−25.
(9) Loudet, A.; Bandichhor, R.; Burgess, K.; Palma, A.; McDonnell, S. O.; Hall, M. J.; O'Shea., D. F. *Org. Lett.* **2008**, *10*, 4771−4774.
(10) Zhao, W.; Carreira, E. M. *Chem.—Eur. J.* **2006**, *12*, 7254−7263.
(11) Christensen, L. P. *Rec. Res. Dev. Phytochem.* **1998**, *2*, 227.
(12) Mishra, A.; Ma, C.-Q.; Bäuerle, P. *Chem. Rev.* **2009**, *109*, 1141.
(13) Rihn, S.; Retailleau, P.; Bugsaliewicz, N.; Nicola, A. D.; Ziessel, R. *Tetrahedron Lett.* **2009**, *50*, 7008−7013.
(14) Han, F.; Chi, L.; Liang, X.; Ji, S.; Liu, S.; Zhou, F.; Wu, Y.; Han, K.; Zhao, J.; James, T. D. *J. Org. Chem.* **2009**, *74*, 1333−1336.
(15) Lakowicz, J. R. *Principles of Fluorescence Spectroscopy*, 2nd ed.; Kluwer Academic/Plenum Publishers: New York, 1999.
(16) Valeur, B. *Molecular Fluorescence: Principles and Applications*; Wiley-VCH Verlag: Weinheim, 2001.
(17) Parson, W. W. *Modern Optical Spectroscopy: With Examples from Biophysics and Biochemistry*; Springer-Verlag: Berlin, Heidelberg, 2007.
(18) Killoran, J.; Allen, L.; Gallagher, J. F.; Gallagher, W. M.; O'Shea, D. F. *Chem. Commun.* **2002**, 1862−1863.
(19) Chen, J.; Reibenspies, J.; Derecskei-Kovacs, A.; Burgess, K. *Chem. Commun.* **1999**, 2501−2502.
(20) Loudet, A.; Bandichhor, R.; Wu, L.; Burgess, K. *Tetrahedron* **2008**, 3642−3654.
(21) Rouxel, C.; Charlot, M.; Mir, Y.; Frochot, C.; Mongin, O.; Blanchard-Desce, M. *New J. Chem.* **2011**, *35*, 1771−1780.
(22) Ginocchietti, G.; Galiazzo, G.; Mazzucato, U.; Spalletti, A. *Photochem. Photobiol. Sci.* **2005**, *4*, 547−553.
(23) Shibata, K.; Katsuyama, I.; Matsui, M.; Muramatsu, H. *J. Heterocycl. Chem.* **1991**, *28*, 161−165.